Geophys. J. Int. (–) –, –

Supplementary information for:
Optimal Stacking of Noise Cross-Correlation Functions

Xiaotao Yang[1,2⋆] (xtyang@purdue.edu), Jared Bryan[3], Kurama Okubo[1,4],

Chengxin Jiang[1,5], Timothy Clements[1,6], and Marine A. Denolle[1,7]

[1] *Department of Earth and Planetary Sciences, Harvard University. Cambridge, MA, USA*
[2] *Now at Department of Earth, Atmospheric, and Planetary Sciences, Purdue University. West Lafayette, IN, USA*
[3] *Department of Earth, Atmospheric, and Planetary Sciences, Massachusetts Institute of Technology. Cambridge, MA USA*
[4] *Now at National Research Institute for Earth Science and Disaster Resilience, Tsukuba, Japan*
[5] *Now at Research School of Earth Sciences, Australian National University. Acton, ACT Australia*
[6] *Now at Earthquake Science Center, United States Geological Survey. Moffet Field, CA USA*
[7] *Now at Department of Earth and Space Sciences, University of Washington, Seattle, WA USA*

Text S1: NCF variability from bootstrapping test

The amplitudes and the standard deviations for different stacking methods could be on significantly different scales, making it hard to directly compare the performance of different methods and the temporal variability by the standard deviations. Therefore, to examine the deviation of the all-time NCF stack for each station pair from the average of the bootstrap mean stacks, we define the deviations index (DI) of the NCF stack for a station pair as:

$$DI = \sum_{i=1}^{M} (|d_i^{all} - d_i^{bootstrap}|/\sigma_i), \tag{S1}$$

where d_i^{all} and $d_i^{bootstrap}$ are the amplitudes of the i^{th} lag-time sample of the all-time stack and bootstrap mean stack, respectively, and σ_i is the standard deviation of the i^{th} sample computed from the bootstrapping test. Fig. S7 shows the distribution of DIs for all station pairs with $\geq$5 NCFs. We observe that most of the DI values are below the baseline of 1.0 (thick line), which means that the overall difference between the all-time and bootstrap mean NCF stacks falls within the standard deviation. The DI values of some station pairs using the Cluster stacking method are above 1.0. The results using the linear and PWS methods show the lowest DIs ranging from 0.01 to 0.05. In summary, taking into account the variation of temporal weighting when stacking, we argue that the all-time stacks are stable representations of the NCFs within the standard deviations.

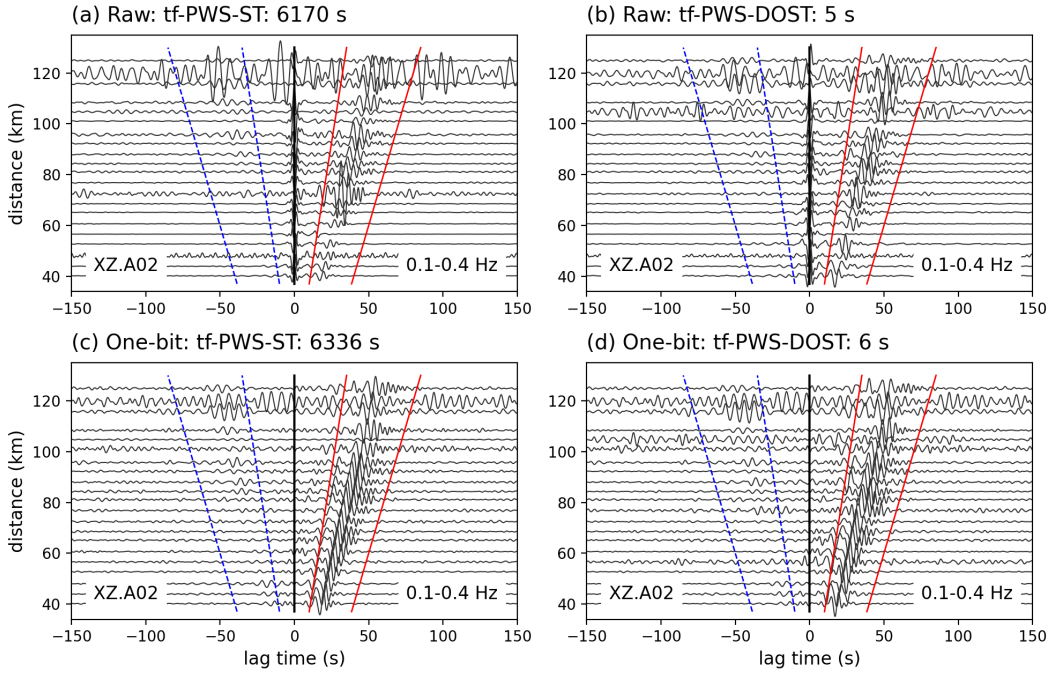

Figure S1. Comparison of stacked noise cross-correlation functions (NCFs) between station XZ.A02 and other stations in the XZ network, using the time-frequency Phase-Weighted Stacking (tf-PWS) method based on the original S-transform (ST; Stockwell et al., 1996) and the discrete orthogonal S-transform (DOST; Stockwell, 2007). We show results using both Raw (top) and One-bit (bottom) NCFs. The number in the title of each panel is the CPU time used in stacking of all station pairs.

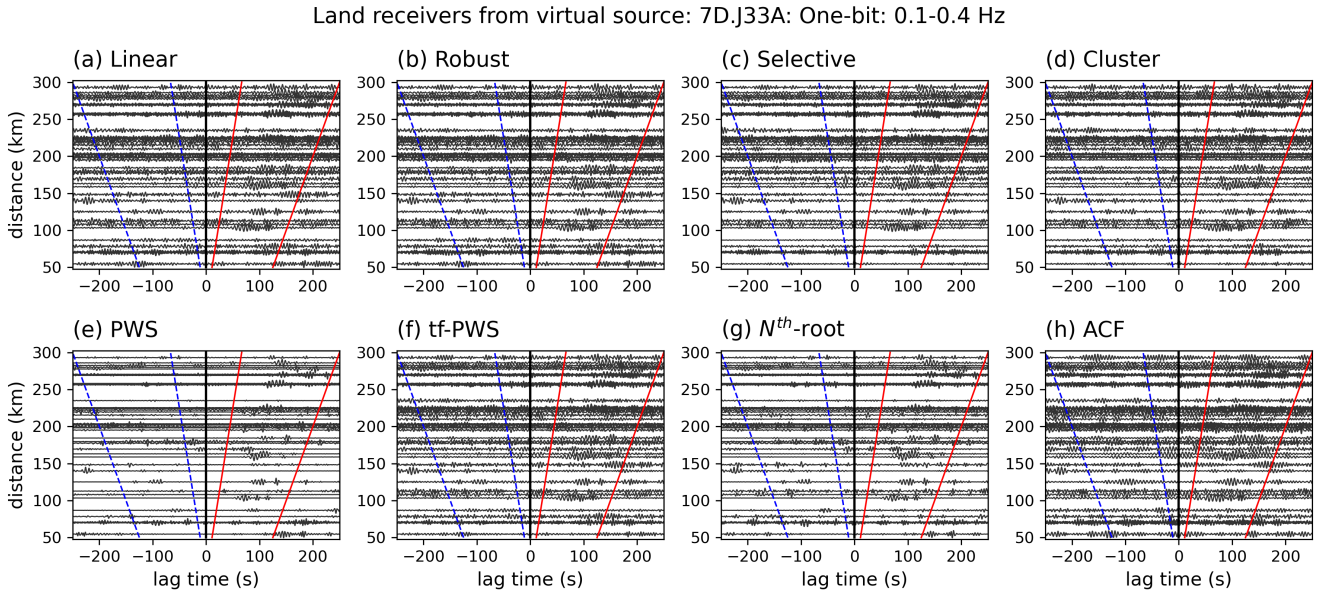

Figure S2. Stacked One-bit noise cross-correlation functions of the Cascadia amphibious array from 7D.J33A to other land receivers using different stacking methods, filtered at 0.1-0.4 Hz. (a-h) The results using the Linear, Robust, Selective, Cluster, PWS, tf-PWS, Nth-root, and ACF stacking methods, respectively. The red solid lines and the blue dashed lines outline the positive-lag signal window and the negative-lag signal window, respectively, used to compute the signal-to-noise ratios in Fig. 7 in the main text. The signal and noise windows are determined with the same method as in Fig. 3a-b in the main text.

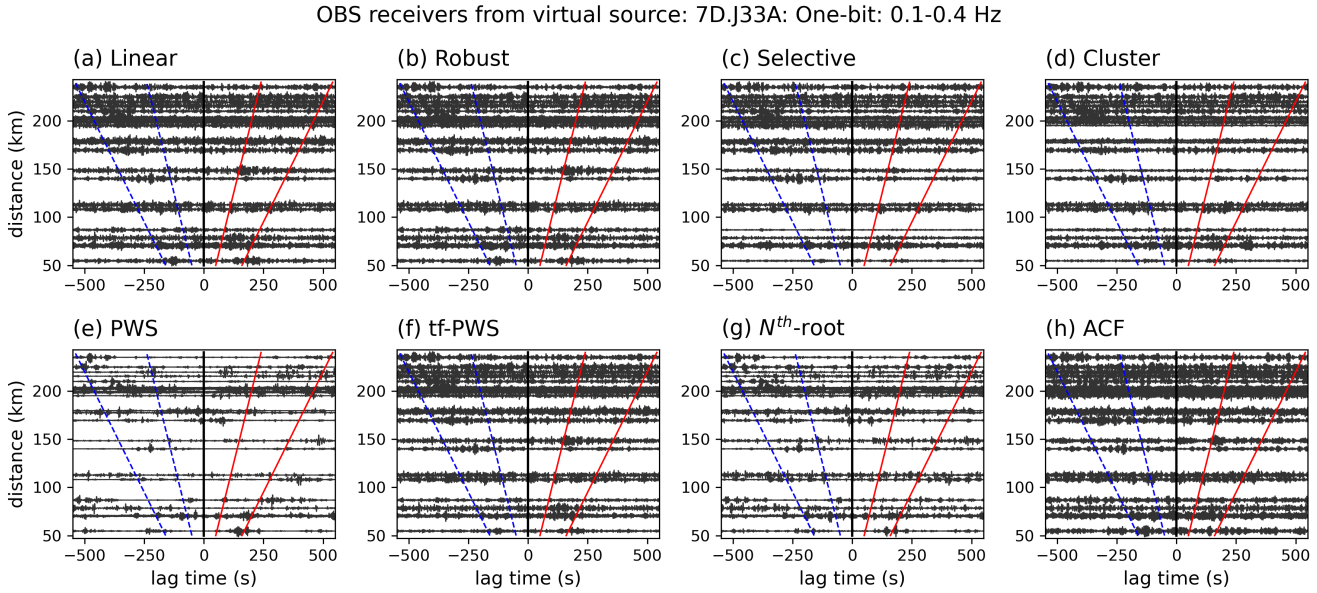

Figure S3. Same as Fig. S2 but for NCFs from 7D.J33A to other Ocean Bottom Seismograph (OBS) receivers. To contain the visually identified ballistic phases from these OBS station pairs, we use a different velocity range (0.5-1.0 km/s) here to predict the signal window of the weakly coherent signals. We extend the window for an additional 60 s after the latest predicted arrival. See Fig. 1 in the main text for locations of the OBS receivers.

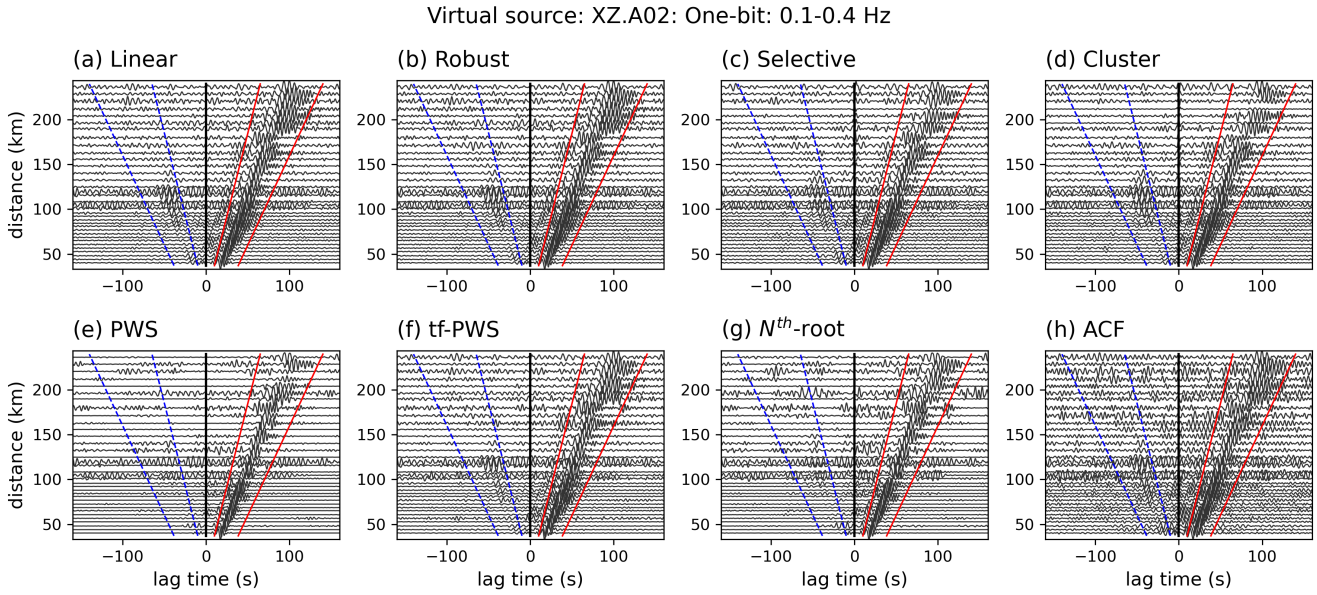

Figure S4. Stacked One-bit NCFs between the XZ.A02 and other receivers, filtered at 0.1-0.4 Hz. (a-h) The results using the Linear, Robust, Selective, Cluster, PWS, tf-PWS, Nth-root, and ACF stacking methods, respectively. The red solid lines and the blue dashed lines outline the positive signal window and the negative signal window, respectively, used to compute the signal-to-noise ratios in Fig. 7 in the main text. The signal and noise windows are determined with the same method as in Fig. 3c-d in the main text. See Fig. 1 in the main text for station locations.

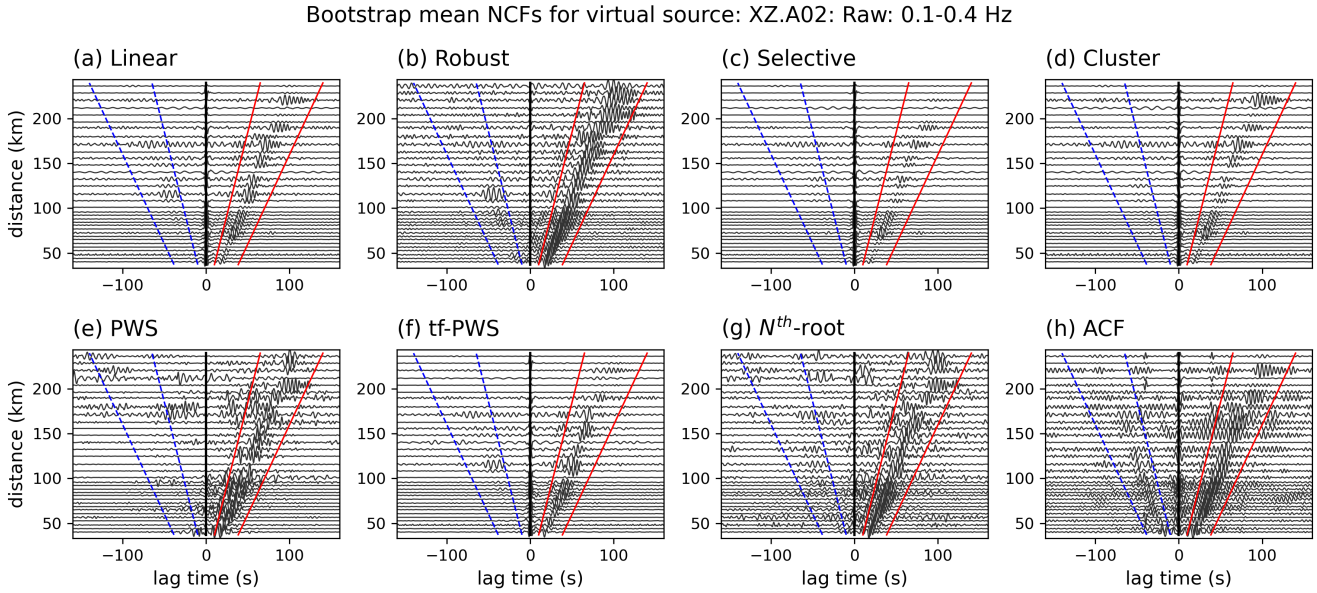

Figure S5. The average of the Raw NCF stacks between XZ.A02 and other receivers filtered at 0.1-0.4 Hz, with bootstrapping of 1000 times and 80% resampling ratio without replacements. (a-h) The results using the Linear, Robust, Selective, Cluster, PWS, tf-PWS, Nth-root, and ACF stacking methods, respectively. The red solid lines and the blue dashed lines outline the positive signal window and the negative signal window, respectively. The signal and noise windows are determined with the same method as in Fig. S4. See Fig. 1 in the main text for station locations.

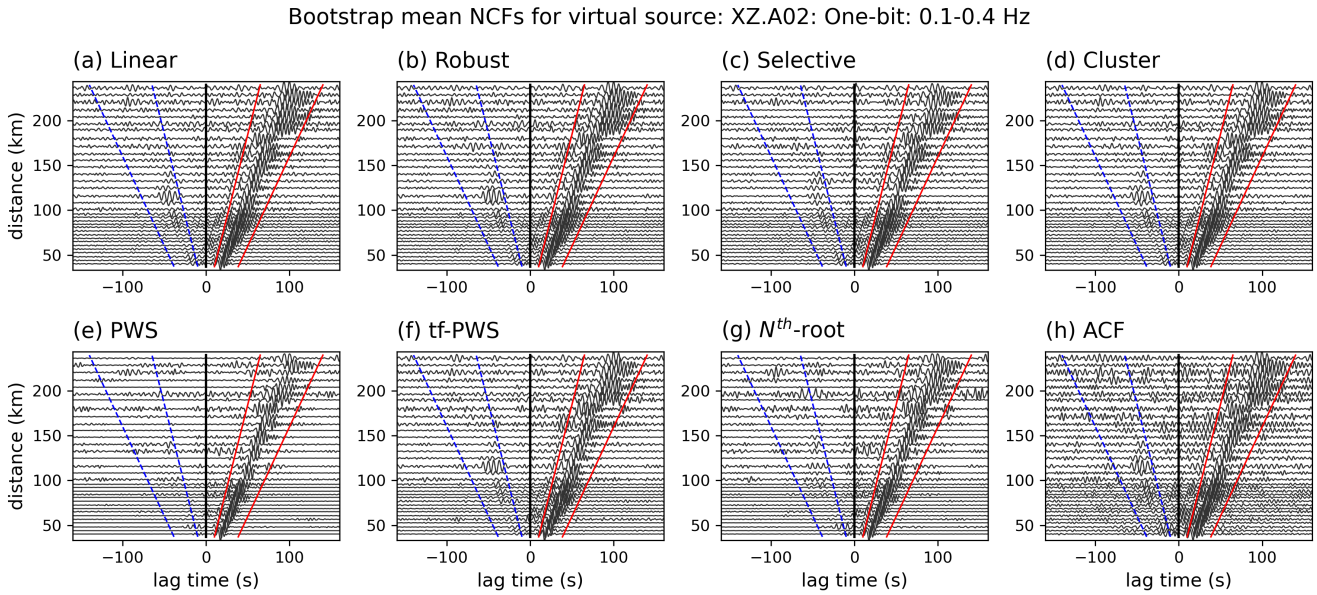

Figure S6. Bootstrap mean NCF stacks same as Fig. S5 but for One-bit NCFs.

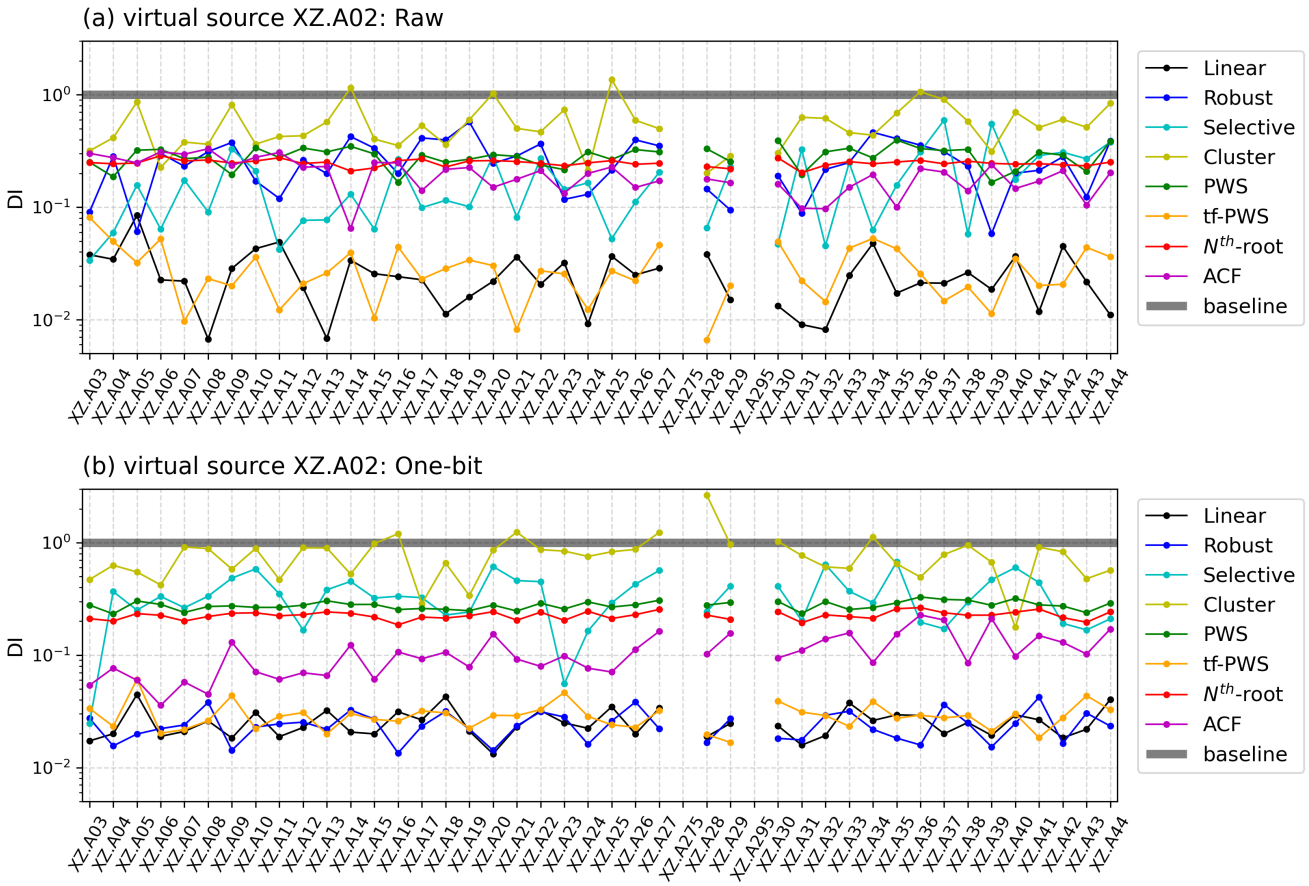

Figure S7. Deviation index (DI) between the all-time NCF stacks and the bootstrap mean NCF stacks for (a) Raw and (b) One-bit NCFs. The deviation index of the NCF stack for each station pair is computed with Equation S1. The thick line shows the baseline value when the difference is comparable to the standard deviation of the bootstrapping test. We only compute the DIs for station pairs with ≥ 5 NCFs.

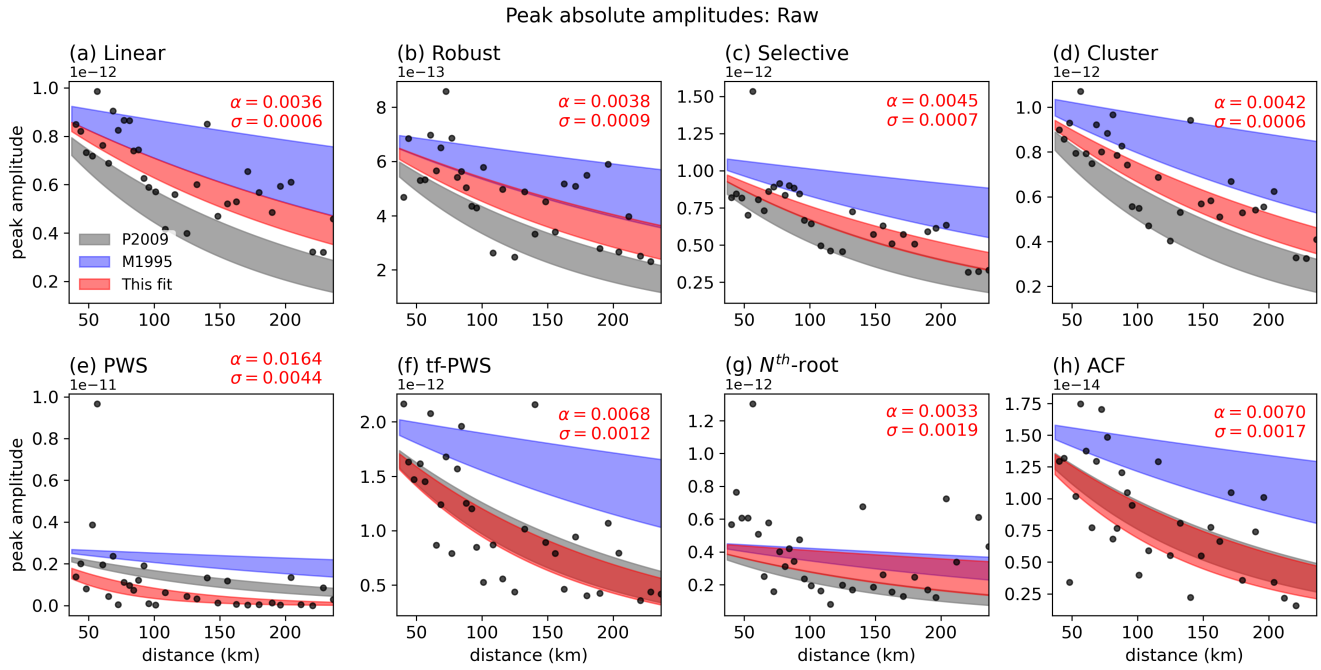

Figure S8. Amplitude fit same as Fig. 14 in the main text but with the mean bootstrap stacks of Raw NCFs as shown in Fig. S5. See Fig. 14 and the main text for amplitude fitting procedures and parameters. The exponential fit from this study is shown as the red shaded area. For reference, we also show the amplitude decay estimated by Prieto et al. (2009) (P2009; α=0.0064$\pm$0.0013; gray shaded area) and Mitchell (1995) (M1995; α=0.002$\pm$0.001; blue shaded area).

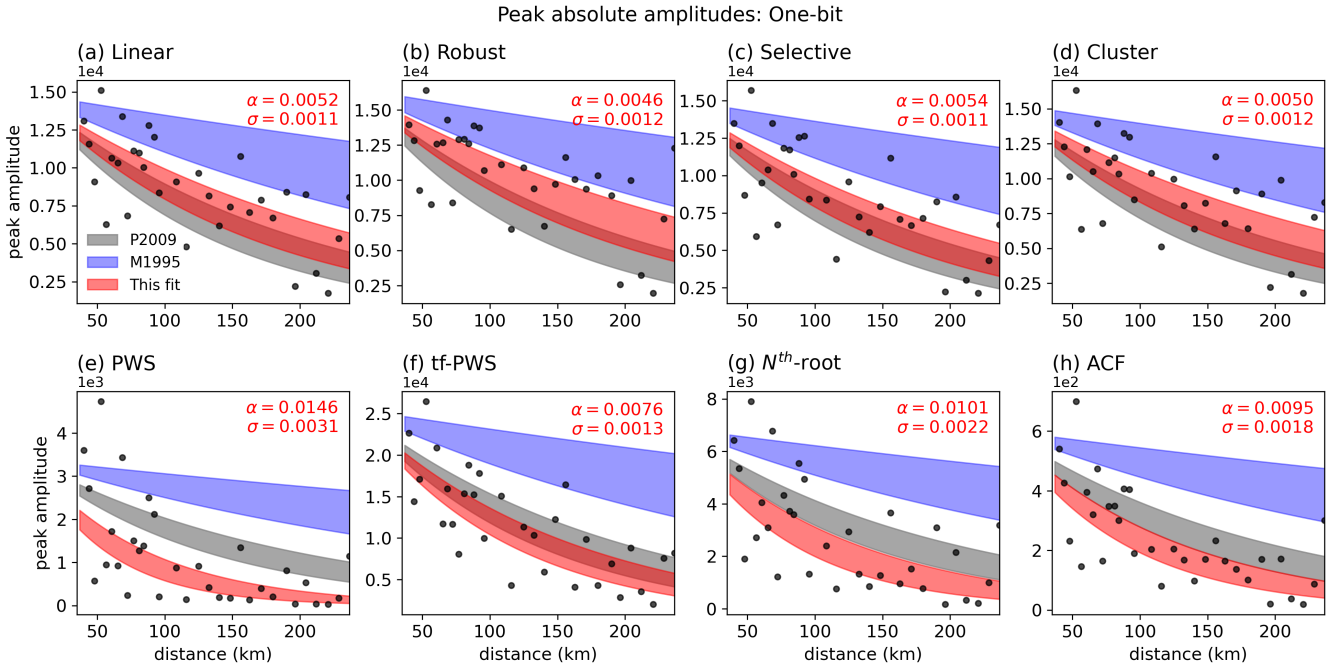

Figure S9. Amplitude fit the same as Fig. S8 but with mean bootstrap stacks of One-bit NCFs (see Fig. S6 for the NCF stacks).

References

Mitchell, Brian J (1995). "Anelastic structure and evolution of the continental crust and upper mantle from seismic surface wave attenuation". In: *Reviews of Geophysics* 33.4, pp. 441–462.

Prieto, G. A., J. F. Lawrence, and G. C. Beroza (2009). "Anelastic Earth structure from the coherency of the ambient seismic field". In: *Journal of Geophysical Research: Solid Earth* 114.7, pp. 1–15. ISSN: 21699356. DOI: 10.1029/2008JB006067.